

Computational Simulation of Turbulent Flow Around Tractor-Trailers

D. O. Redchyts¹, E. A. Shkvar^{2,*} and S. V. Moiseienko³

Abstract: A method to evaluate the properties of turbulent flow in proximity to the vehicle and close to the ground surface has been elaborated. Numerical simulations have been performed on the basis of the Unsteady Reynolds-averaged Navier-Stokes equations (URANS) written with respect to an arbitrary curvilinear coordinate system. These equations have been solved using the Spalart-Allmaras differential one-parametric turbulence model. The method of artificial compressibility has been used to improve the coupling of pressure and velocity in the framework of a finite volume approach. Time-averaged distributions of pressure fields, velocity components, streamlines in the entire area and near the tractor-trailer, as well as integral and distributed characteristic parameters (such as coefficients of pressure, friction and drag force) are presented. According to our results, the turbulent flow accelerates in the area of the tractor cabin and in the gap between surfaces. Above the driver's cabin, a pressure drop occurs due to a sharp acceleration of flow in this area. Downstream, pressure is restored and becomes almost constant in proximity to the edge of the trailer. The dimensions of the separation area exceed the length of the transport system several times. Though agreement with experimental results is relatively limited due to the two-dimensional nature of the numerical simulations, the present approach succeeds in identifying the main physical effects involved in the considered dynamics. It might be used in future studies for initial approximate assessments of the influence of the vehicle shape on its aerodynamic characteristics.

Keywords: High-speed vehicle, tractor-trailer, turbulent flow, ground effect, numerical modelling, aerodynamic characteristics.

1 Introduction

High-speed ground vehicles, including trains, are an intensively developing mode of modern transport. Due to the importance of their efficiency improvement, the research area in this field is particularly wide (from magnetic-levitation or hyperloop principles application to the optimization of bogie design, gap area between cars or the connection of two cabins, pantographs and so on), but the most active area of study is high-speed train aerodynamics

¹ Institute of Transport Systems and Technologies of Ukrainian National Academy of Science, Dnipro, 49005, Ukraine.

² College of Engineering, Zhejiang Normal University, Jinhua, 321004, China.

³ Kherson National Technical University, Kherson, 73008, Ukraine.

* Corresponding Author: Eugene Shkvar. Email: shkvar.eugene@qq.com.

Received: 12 July 2019; Accepted: 21 October 2019.

because even in cases of crosswind absence (symmetric streamline), aerodynamic drag dominates in comparison with other mechanical resistance components if the vehicle speed exceeds 200 km/h. In particular, the aerodynamic drag of a typical high-speed wheel train at a cruising speed of 300 km/h is approximately 85% [Gawthorpe (1978)] of the train's total drag. However, even for a train speed of around 100 km/h, the aerodynamic drag component begins to play a significant role in the total drag and should be taken into account. Various experimental and theoretical studies [Baker (2014), Shkvar, Jamea, Cai et al. (2018)] have determined that the pressure and skin friction components of high-speed train aerodynamic drag in the case of a symmetric streamline can be qualitatively predicted numerically, typically by applying finite-volume methods and on the basis of sufficiently simple isotropic models of turbulence such as Spalart-Allmaras' model of a well-optimized train shape. Moreover, as Shkvar et al. [Shkvar, Jamea, Cai et al. (2018)] showed, these distributions are slightly dependent on the chosen face of the train body; most of a train's length (approximately 85%), except for the head and tail cabins, is characterized by the absence of a pressure change in the longitudinal direction; the skin friction coefficient C_f can be qualitatively approximated by well-known empirical dependencies, proposed for a turbulent streamline of a smooth flat plate in the case of particularly high significances of Reynolds number Re_x by Schlichting $C_f=[2 \lg(Re_x)-0.65]^{-2.3}$, Nikuradze $C_f=0.02296(Re_x)^{-0.139}$, Schultz-Grunow $C_f=0.37 [\lg(Re_x)]^{-2.584}$ or effectively predicted numerically on the basis of the boundary layer equations. Hence, the boundary layer that develops around the most of streamlined surface area of a high-speed train body is quite similar to the 2D case and can be approximated by flow over a flat plate of an equivalent area and without a pressure gradient; this approach can significantly simplify and improve the efficiency of flow parameter prediction. Moreover, in many practical cases, the flow modelling can be realized with appropriate engineering application accuracy level only in the train symmetry plane. Nevertheless, even in this favourable case, it is important to improve the numerical methodology in order to provide further train shapes and their streamlined surface optimisation on the basis of different flow control techniques. In the case of other high-speed vehicles, this conclusion applies even for lower movement speeds because of a more complex shape geometry and corresponding flow structure. In the case of trucks, the decrease of drag is directly connected with the economy of diesel fuel consumption that is relevant in the conditions of market competition of freight. For a tractor-trailer, the fuel consumption for overcoming the drag force at speeds of the order of 80 km/h becomes comparable to the fuel consumption for rolling friction of the wheels. At a speed of 110 km/h, fuel consumption to overcome the aerodynamic drag is already 65% of the total consumption. Therefore, 20-25% of drag reduction can lead to a decrease in fuel consumption of 10-15% [Storms, Ross, Heineck et al. (2001); Salari and McWherter-Payne (2003)]. In addition, because trucks are not particularly streamlined, in contrast to high-speed trains, they are more informative objects for verification and validation of the models and methods for numerical prediction of aerodynamic properties of different vehicles. In comparison with trains, the aerodynamic drag of trucks is characterized by the pressure drag component dominating due to their smaller length and the presence of a large tail-separating zone with intensive vortical systems in the near wake [Kim, Kim and Lee (2017), Peng, Wang, Yang et al. (2018)]. One more important factor for all high-speed ground vehicles is

the ground effect, which plays an important role in the generation and further development of wake flow dynamics and, as a result, additional energy dissipation and drag. However, its adequate simulation in physical experiments in the case of high-speed movement is practically difficult or unrealizable; therefore, the numerical modelling methods demonstrate in this case their significant advantages, but for such complex kinds of flow with intensive vortical motion in the near-wake region, they can require careful adjustment and verification. Hence, the analysis of applicability, assessment of possibilities and further development of computational methods of turbulent flow modelling around vehicles that have different geometries and that are moving in the neighbourhood of the ground surface are important both in theoretical and applied aspects. Computational fluid dynamics (CFD) is one of the key components of the modern design process in research associated with the aerospace industry, propulsion engineering and wind energy due to the lower cost of numerical investigations compared with physical experiments. It effectively enables the reproduction of real physical processes, better understanding of their interaction and provides recommendations for aerodynamic optimization of the designed device or its separate elements. Today, the optimization of the aerodynamic form of tractor-trailers is carried out by multiple wind-tunnel tests. In the near future, CFD calculations could significantly reduce the number of required wind-tunnel tests and, as a result, effectively minimize the final cost of the developed product.

2 Brief description of chosen object of study and existing experimental data

For computer simulation of a turbulent flow around a vehicle near a screen surface, a ground transportation system (GTS) configuration was chosen, reflecting the geometry of a tractor with a trailer (Fig. 1). This configuration was selected because it had been studied previously by the Ames Research Center (ARC) and SANDIA [Salari and McWherter-Payne (2003)]. There are reliable experimental data for this object, and there are complex physical effects from the point of view of fluid and gas mechanics. An experimental study of the ground transportation system was conducted at ARC [Storms, Ross, Heineck et al. (2001)]. The mirrors, wheels, gap between the tractor and the trailer, and small structural elements are not considered in the simplified configuration. Experimental data include a set of integral and distributed characteristics, most of which are the coefficients of pressure and friction.

3 Motivation and research goals

- Check the assumption regarding the applicability of a two-dimensional model for calculating the flow field in the symmetry plane of the vehicle.
- In the case of a positive result of the previous item, to be able to quickly assess the aerodynamic coefficients of the vehicle when changing its shape.
- Extend the area of application of the developed CFD package to a new class of modelling problems.

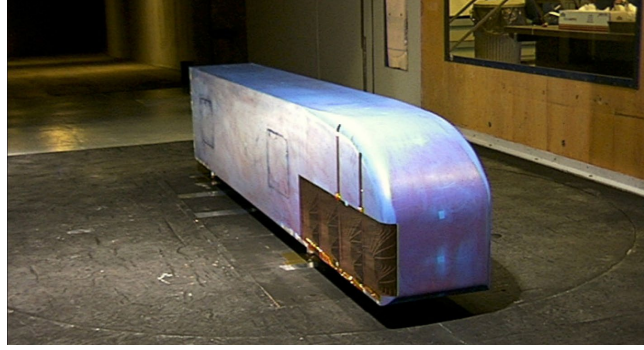


Figure 1: Experimental model of a tractor-trailer [Storms, Ross, Heineck et al. (2001)]

4 Statement of the problem of numerical simulation

The methodology developed in this paper is based on the assumption of low-speed air movement at low Mach numbers ($M < 0.3$), where the airflow can be considered to be an incompressible fluid due to neglecting the compressibility effects. The URANS equations for an incompressible fluid are used in order to study the aerodynamic processes of the ground transport system:

$$\nabla \mathbf{u} = 0 \quad (1)$$

$$\frac{\partial \mathbf{u}}{\partial t} + (\mathbf{u} \cdot \nabla) \mathbf{u} = -\frac{1}{\rho} \nabla p + \nabla [(\nu + \nu_t) \nabla \mathbf{u}] \quad (2)$$

where ∇ -Hamiltonian operator, t -time, \mathbf{u} -mean speed vector, p -pressure, ρ -density, ν and ν_t -molecular and turbulent kinematic viscosity coefficients, respectively.

The system of equations is written in dimensional form for physical variables in the Cartesian coordinate system. This form of writing the Navier-Stokes Eqs. (1) and (2) is a consequence of the integral laws of conservation of mass and momentum.

Aerodynamic moment is calculated using the expression:

$$Q = \iint_S [(x - x_0) F_y - (y - y_0) F_x] dS \quad (3)$$

$$F_x = -p \cos(\bar{\mathbf{n}}, \bar{\mathbf{i}}) + \tau \cos(\bar{\mathbf{t}}, \bar{\mathbf{i}}) \quad (4)$$

$$F_y = -p \cos(\bar{\mathbf{n}}, \bar{\mathbf{j}}) + \tau \cos(\bar{\mathbf{t}}, \bar{\mathbf{j}}) \quad (5)$$

where F_x , F_y -projections of aerodynamic forces on the axes of Cartesian coordinates, referred to the elementary area; x , y -Cartesian coordinates; x_0 , y_0 -the coordinates of the axis of rotation, relative to which the aerodynamic moment is determined; S -surface of the streamlined body; $\tau = \mu(\partial U_\tau / \partial l_n)$ -shear stress; U_τ -tangential component of the velocity vector; l_n -normal distance to surface; μ -coefficient of dynamic viscosity; $\bar{\mathbf{n}}$ - surface normal vector; $\bar{\mathbf{t}}$ -tangent vector to the surface; $\bar{\mathbf{i}}$, $\bar{\mathbf{j}}$ -Cartesian basis vectors.

For the closure of the URANS equations, the Spalart-Allmaras (SA) differential one-parametric turbulence model Eq. (2), designed primarily for problems of external subsonic aerodynamics, was used.

The standard Spalart-Allmaras turbulence model is designed to determine the dimensional kinematic coefficient of turbulent viscosity:

$$\nu_t = \tilde{\nu}_t \cdot f_{v1} \quad (6)$$

where $f_{v1} = \chi^3 / (\chi^3 + c_{v1}^3)$ -kinematic viscosity damping function $\chi = \tilde{\nu}_t / \nu$, $\tilde{\nu}_t$ -work variable. The equation for the definition $\tilde{\nu}_t$ in the Spalart-Allmaras model is

$$\frac{D\tilde{\nu}_t}{Dt} = c_{b1} \tilde{S} \tilde{\nu}_t + \frac{1}{\sigma} \nabla \cdot [(\nu + \tilde{\nu}_t) \nabla \tilde{\nu}_t] + \frac{c_{b2}}{\sigma} \nabla^2 \tilde{\nu}_t - f_w \left(\frac{c_{b1}}{k^2} + \frac{1 + c_{b2}}{\sigma} \right) \left(\frac{\tilde{\nu}_t}{d} \right)^2 \quad (7)$$

The first term on the right-hand side of Eq. (7) is the source term for the generation of turbulence:

$$\tilde{S} \equiv f_{v3} W + \frac{\tilde{\nu}_t}{k^2 d^2} f_{v2}, \quad W = \sqrt{2W_{ij}W_{ij}} \quad (8)$$

where $W_{ij} = 0.5(\partial u_i / \partial x_j - \partial u_j / \partial x_i)$ -vorticity tensor.

The function f_{v2} is determined by the ratio:

$$f_{v2} = 1 - \frac{\chi}{1 + \chi f_{v1}} \quad (9)$$

The second and third terms on the right-hand side of Eq. (7) are responsible for the dissipation of turbulence. The fourth term specifies the destruction of turbulence near a solid wall and contains the function:

$$f_w = g \left[\frac{1 + c_{w3}^6}{g^6 + c_{w3}^6} \right]^{1/6} \quad (10)$$

where $g = r + c_{w2}(r^6 - r)$, $r = \frac{\tilde{\nu}_t}{\tilde{S} k^2 d^2}$. Here d -distance to the nearest wall. Constant

values: $k = 0.41$ -Kármán constant, $\sigma = 2/3$ -turbulent Prandtl number, $c_{b1} = 0.1355$, $c_{b2} = 0.622$, $c_{v2} = 5.0$, $c_{w2} = 0.3$, $c_{w3} = 2$, $c_{v1} = 7.1$, $f_{v3} = 1$.

For the determination of initial conditions, the parameters of the undisturbed flow were set in the entire computational domain. Non-reflective boundary conditions were applied on the outer boundary, for their calculation the method of characteristics was used. A sticking condition was imposed on the surface of a solid body. In the turbulence model, the value of the working variable on the body was set to zero $\tilde{\nu}_t = 0$, at the inflow boundary condition it was $\tilde{\nu}_t = 0.1$, and the Neumann condition was set at the outflow boundary.

The length of the GTS model is 2.47 m, which was chosen as the characteristic size (equivalent to 1.0 in dimensionless values). The height is 0.44 m (0.182). The front rounding (driver's cabin) is a quarter of an ellipse, the small radius is 0.22 m (0.08975),

and the large radius is 0.38 m (0.15385). The gap between the screen and the model is 0.07 m (0.0314). The flow velocity in the wind tunnel is 78 m/s (1.0). The Reynolds number, calculated by the length and velocity of the free-stream flow, is $1.53 \cdot 10^7$.

The computational grid is a Chimera-type grid consisting of two blocks. The total number of nodes is 10^5 (Fig. 2). The first block is an O-grid associated with the body, and the second is a rectangular grid that is adjacent to the surface (screen). The first dimensionless grid step is 10^{-6} . The main purpose of the generated computational grid around GTS was to allow a turbulent boundary layer on the GTS surface and in the near wake. This specification requires that approximately 10 grid nodes in the direction normal to the surface are located inside the viscous sublayer. In the near wake behind the GTS surface, the grid cells were close to orthogonal and with a small aspect ratio. In the far wake and in the region of the unperturbed flow, the aspect ratios are no longer essential.

Another important goal of this research was to examine the assumption that the two-dimensional model is applicable for calculating the flow field in the vehicle symmetry plane. The constructed grid in the presence of strong local changes in its cell parameters demonstrated both stable convergence of the iterative solution process and satisfactory agreement of the predicted integrated and distributed flow characteristics with the corresponding experimental data. Hence, for the described research, the grid parameter changes and, in particular, the cell aspect ratio were not controlled explicitly.

The dimensionless time step is 10^{-2} due to the requirement to solve the considered problem in a stationary statement and the advantages of the developed numerical method, containing a pseudo-time iteration without any factorization and linearization in physical time (described below).

5 Numerical method

The system of initial equations was written in an arbitrary curvilinear coordinate system. The coupling of the pressure and velocity fields was carried out using the method of artificial compressibility modified to calculate non-stationary problems [Rogers and Kwak (1991)]. The structured grids were used to create a discrete analogue of the initial equations, and the multi-block computing technologies were used in nonsimply connected areas. The dimension of individual intersecting grids (blocks) is not interconnected. Such an approach made it possible to develop a unified methodology for calculating viscous fluid flows around bodies of complex geometric shape.

The integration of the system of initial equations was carried out numerically using the finite volume method. For convective terms, the upwind Rogers-Kwak approximation was used on the basis of the third-order Roe scheme. In turbulence models, the TVD scheme with a third-order ISNAS flow limiter was used to approximate convective terms. The derivatives in viscous terms were approximated by a second-order central difference scheme. For equations solving the algorithm, based on a three-layer implicit scheme with subiterations in pseudo-time of the second order of accuracy in physical time, was used. The obtained block-matrix system of linear algebraic equations was solved by the generalized minimal residual (GMRES) method with ILU (k) preconditioning.

6 Specialized CFD package

A specialized CFD package, developed by Redchyts [Redchyts (2009)], was applied by the author's team for this research program. This software allows to effectively and flexibly reach the necessary level of compromise between the required computational resources and the quality of results. The developed basis of computational methodology provides a complete approach for CFD based on the Navier-Stokes equations, including several differential turbulence models, as well as a multi-block approach for the flows in multiply connected domains. The designed CFD package allows the problem of dynamics and aerodynamics to be solved, including electrodynamics processes, electrochemistry, multiphase fluids, combustion processes and plasma kinetics. The results enabled the formulation of new technical ideas, obtain new understanding about the physics of flow separation and methods for its control and reproduce the real structure of different flow types over a wide speed range.

The developed specialized CFD package, similar to other comparable commercial and opensource software, consists of three typical principal elements: preprocessor, computing core and postprocessor. The preprocessor is responsible for the formation of the original geometry and the creation of discrete space. The computational core integrates the equations. The postprocessor is used for visualization of scalar and vector values, processing the integral characteristics over time and creating an animation of the flow fields using a built-in visualizer.

7 Results and discussion

The physical features of the flow structure are highlighted, and the pressure, lift and drag coefficients are analyzed as a result of the computations of turbulent flow around a tractor-trailer near the surface. The distributions of pressure fields (Fig. 3(a)), components of speed (Fig. 3(b)), streamlines in the entire area and near the tractor with a trailer (Fig. 4), as well as values of integral and distributed characteristics (Fig. 5) were obtained. The resulting picture of the flow around the model of a tractor-trailer is unsteady. This model is associated with poorly streamlined bodies. The dimensions of the separated zone exceed the length of the considering ground transportation system by several folds.

The flow accelerates in the cabin area and in the gap between the screens (Fig. 1) when flowing around the tractor with a trailer. Above the driver's cabin, a pressure drop occurs due to an intensive acceleration of flow in this area. In the downstream, the pressure is restored and becomes almost constant to the edge of the trailer. A recirculation current with a flow opposite to the main flow is formed in the wake. The vortices in the tail part of the model alternately descend from the top and bottom surfaces. The presence of a massive vortical system leads to a significant pressure decrease. The large pressure drop between the frontal and tail parts of the tractor results in a significant pressure drag increase.

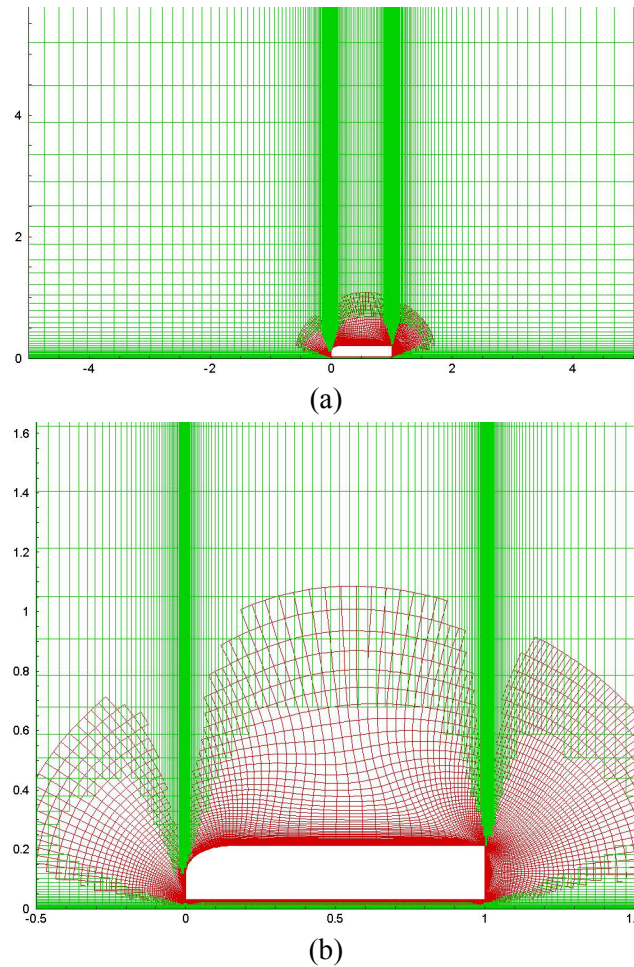


Figure 2: Calculated grid in the entire area (a) and near the tractor-trailer (b)

A uniform flow is realized in the gap, similar to the flow in the channel, except for a small area near the cabin. In the bottom part, the flow structure is close to the Karman vortex shedding. Flow separation occurs at the bottom of the trailer from sharp edges, as well as in the lower part of the cabin near the surface. The flow separation is clearly illustrated by the streamlines (Fig. 4).

The distribution of the pressure coefficient over the model surface is obtained (Fig. 5(a)). The noticeable difference in pressure ratio between the experimental and calculated data on the upper surface is associated with the two-dimensional formulation of the problem. The direction of flow spreading is limited, in contrast to the three-dimensional formulation of the problem. The weak recovery of pressure at the tail of the trailer is due to the properties of the Spalart-Allmaras turbulence model, which generates excessive values of the turbulent viscosity in the separated zone.

This effect also manifests itself in the distribution of the friction coefficient in the front part of the model (Fig. 5(b)). At the same time, the general distribution of the friction

coefficient is in satisfactory agreement with the experimental data. The calculated value of the aerodynamic drag coefficient is 0.37, the corresponding experimentally obtained result is 0.27 [Storms, Ross, Heineck et al. (2001)]. The main reason for this deviation is the 2D statement of the problem of numerical modelling.

A comparison of the results of numerical simulation with the calculated SANDIA data [Salari and McWherter-Payne (2003)] (Figs. 6 and 7) was carried out. The drag coefficient of a tractor with a trailer obtained using the SACCARA CFD code developed by SANDIA is 0.42. There is a qualitative (Figs. 6 and 7) and quantitative agreement of the results with the calculated data of SANDIA. Small deviations are the result of differences in gap. In addition, the calculations performed in [Salari and McWherter-Payne (2003)] were carried out with the Reynolds number $Re_w=1.6e6$ (calculated from the width of the model), and in this work, $Re_w=2 \cdot 10^6$ (calculated from the model width) corresponds to $Re_l=1.53 \cdot 10^7$ (calculated from the model length). Thus, this paper presents only a qualitative comparison of the flow pattern of the GTS model with the calculations of [Salari and McWherter-Payne (2003)] (Figs. 6 and 7). A quantitative comparison was made with the above-mentioned results of experimental studies [Storms, Ross, Heineck et al. (2001)] (Fig. 5).

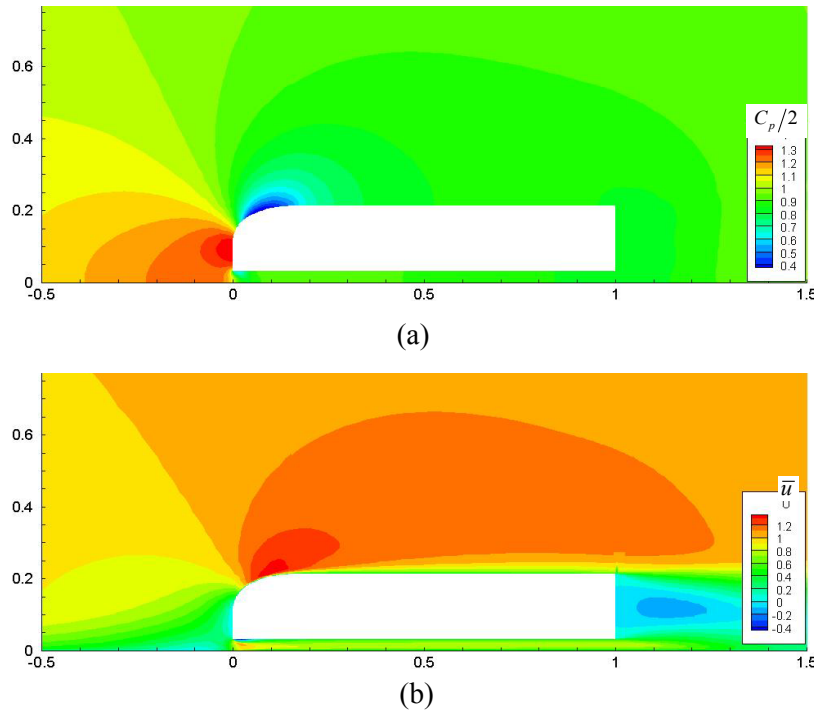


Figure 3: Distribution of dimensionless pressure (a) and x-component of velocity (b) around a tractor-trailer

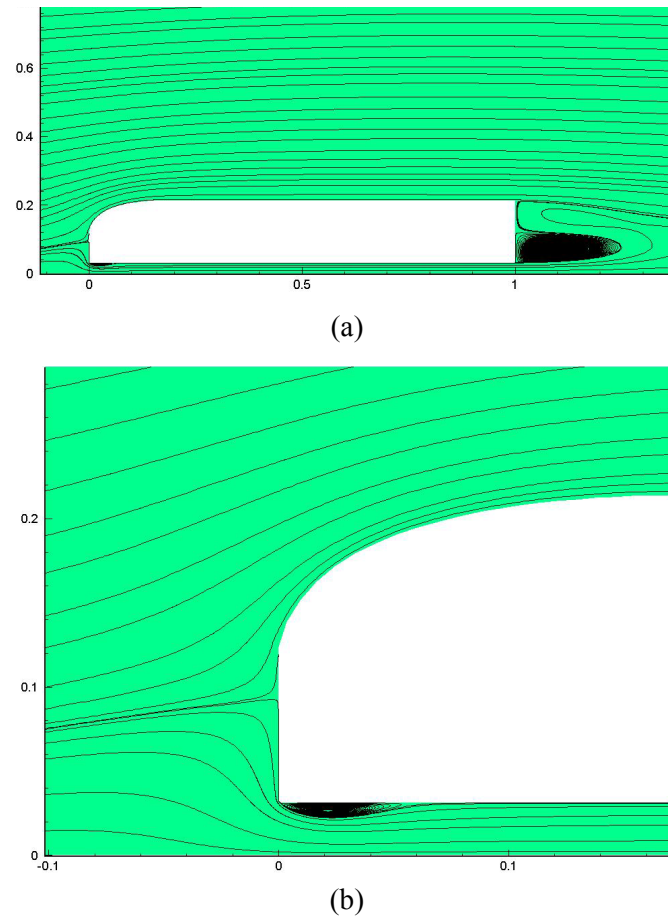
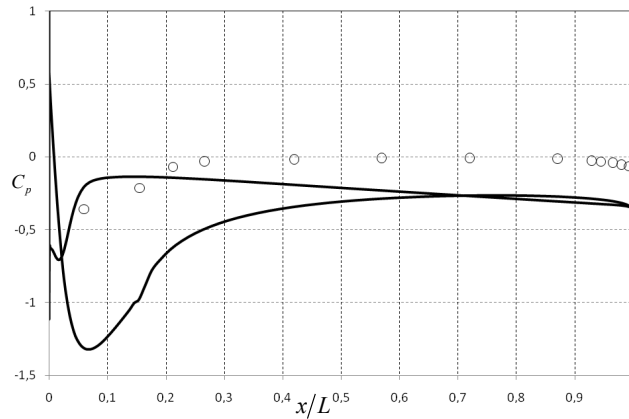


Figure 4: Distribution of streamlines in the entire area (a) and near the cabin of a tractor-trailer (b)

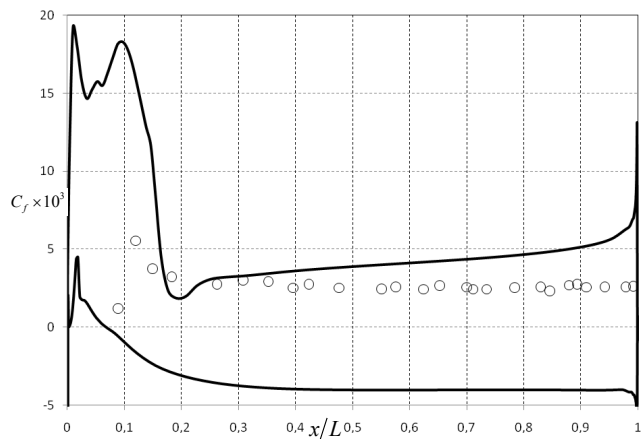
8 Conclusion

Modelling of turbulent flow over the vehicle contour in the ground surface neighbourhood was carried out. The physical features of the flow structure around the vehicle were highlighted, and an analysis of the coefficients of pressure, friction and drag force was performed. A comparative analysis of the integral and distributed aerodynamic characteristics of the contour of the vehicle with experimental and computed data was performed. The applicability of the developed specialized CFD package to the aerodynamics of ground transportation systems was shown. The two-dimensional formulation of the problem allows to identify the main physical effects of the flow and obtain rapid assessments of the influence of the vehicle shape on its aerodynamic characteristics. The presented numerical results were obtained for a tractor-trailer configuration, but the elaborated computational methodology and corresponding CFD software can be applied without any modifications for a wide range of vehicle configurations, including high-speed trains. Further research will be directed to verification

of the 3D version of the developed methodology and improvement of its computational efficiency due to parallel algorithm implementation.

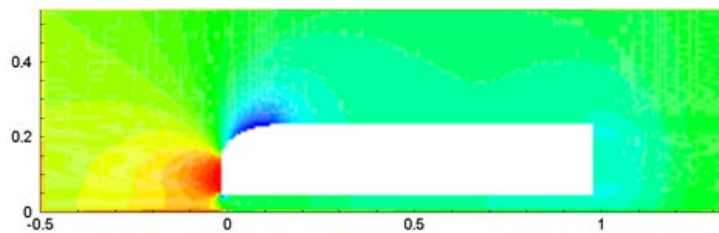


(a)

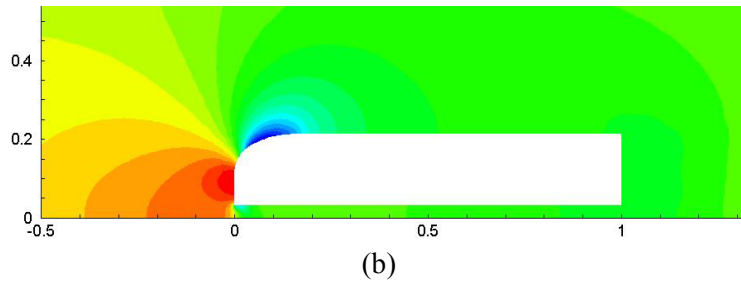


(b)

Figure 5: Distribution of pressure (a) and friction (b) coefficients over the top and bottom surfaces of a tractor-trailer (a-experiment [Storms, Ross, Heineck et al. (2001)], b-present work)

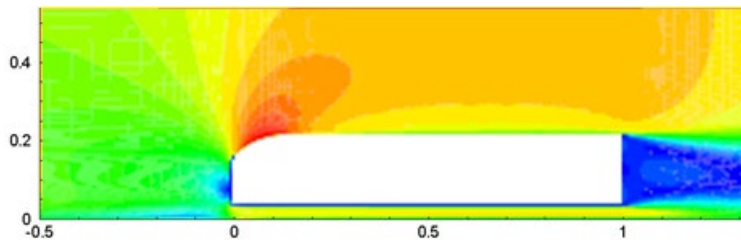


(a)

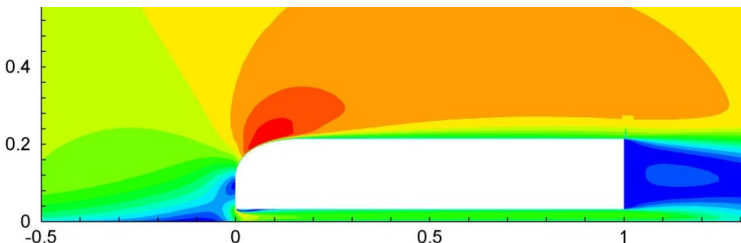


(b)

Figure 6: Turbulent flow around a car model with a trailer. Isobars (a-calculation [Salari and McWherter-Payne (2003)], b-present work)



(a)



(b)

Figure 7: Turbulent flow around a car model with a trailer. Isomachs (a-calculation [Salari and McWherter-Payne (2003)], b-present work)

Conflicts of Interest: The authors declare that they have no conflicts of interest to report regarding the present study.

References

- Baker, C.** (2014): A review of train aerodynamics part 1-Fundamentals. *Aeronautical Journal*, vol. 118, no. 1201, pp. 1-41; Part 2-Applications. *Aeronautical Journal*, vol. 118, no. 1202, pp. 1-56.
- Gawthorpe, R. G.** (1978): Aerodynamics of trains in the open air. *Railway Engineer International*, vol. 3, no. 3, pp. 7-12.
- Kim, J. J.; Kim, J.; Lee, S.** (2017): Substantial drag reduction of a heavy truck vehicle using gap fairings. *Journal of Wind Engineering & Industrial Aerodynamics*, vol. 171, pp. 93-100.

- Peng, J.; Wang, T.; Yang, T.; Sun, X.; Li, G.** (2018): Research on the aerodynamic characteristics of tractor-trailers with a parametric cab design. *Applied Sciences*, vol. 8, no. 5, pp.791-811.
- Redchys, D.** (2009): Numerical simulation of separated flows based on unsteady navier-stokes equations. *Scientific Statements of Belgorod State University. Series Mathematics Physics*, vol. 17, no. 13, pp. 118-146.
- Rogers, S. E.; Kwak, D.** (1991): An upwind differencing scheme for the incompressible navier-stokes equations. *Journal Numerical Mathematics*, vol. 8, pp. 43-64.
- Salari, K.; McWherter-Payne, M. A.** (2003): *Computational Flow Modeling of A Simplified Integrated Tractor-Trailer Geometry*. Department of Energy.
- Spalart, P. R.; Allmaras, P. R.** (1992): A one-equation turbulence model for aerodynamic flow. *AIAA Paper*, vol. 12, pp. 439-478.
- Storms, B. L.; Ross, J. C.; Heineck, J. T.; Walker, S. M.; Driver, D. M. et al.** (2001): An experimental study of the ground transportation system (GTS) model in the NASA ames 7- by 10-ft wind tunnel. *NASA TM-2001-209621*, pp. 26.
- Shkvar, Y. O.; Jamea, A. S. J. E.; Cai, J. C.; Kryzhanovskiy, A. S.** (2018): Effectiveness of blowing for improving the high-speed trains aerodynamics. *Thermophysics and Aeromechanics*, vol. 25, no. 5, pp. 675-687.